Displacement-Based Design of Supplemental Dampers for Seismic Retrofit of a Framed Structure

Jinkoo Kim[1] and Hyunhoon Choi[2]

Abstract: The procedure of direct displacement-based design (DBD), presented in the SEOAC *Blue Book*, was modified to evaluate the seismic performance of existing structures. Then an optimum number of velocity-dependent supplemental dampers, such as viscous and viscoelastic dampers, required to reduce the seismic response of existing structures to a given performance limit state was evaluated. The proposed method was applied to seismic performance evaluation and performance-based seismic retrofit of ten- and 20-story steel frames, and the final design was verified by time history analyses using artificial earthquake records generated based on the design spectrum. According to the analysis results, the performance points evaluated by the proposed method match well with those computed by time-history analyses, and the maximum displacements of the model structures retrofitted by the supplemental dampers corresponded well to the given target values.

DOI: 10.1061/(ASCE)0733-9445(2006)132:6(873)

CE Database subject headings: Displacement; Seismic design; Earthquakes; Damping; Performance characteristics; Evaluation.

Introduction

The energy dissipation devices are known to directly increase the seismic energy dissipation capability of structures (Soong and Dargush 1997). Specifically the velocity-dependent supplemental dampers, such as viscous dampers (VDs) and viscoelastic dampers (VEDs), are highly effective in the velocity sensitive region of a response spectrum, in which maximum acceleration of a structure decreases significantly as the damping in the structure increases.

For seismic retrofit of an existing structure using supplemental dampers in accordance with the philosophy of the performance-based seismic design (PBSD), the appropriate size and location of supplemental dampers need to be determined so that the performance objectives are satisfied. A traditional procedure of determining the size and location of supplemental energy dissipating devices starts from selection of trial values based on the engineer's expertise. Then dynamic or static analysis is performed to check whether the given performance objective is satisfied. For this purpose ATC-40 (ATC 1996) and FEMA-273 (FEMA 1997a) (later developed into FEMA-356) provide nonlinear static analysis procedures incorporating energy dissipation devices. If the analysis result is not satisfactory, the structure is analyzed again after changing the amount or location of the added dampers. This trial-and-error process is repeated until the optimum number of supplemental dampers to satisfy the given performance acceptance criteria is finally reached. However this general practice of carrying out a series of trial and error processes can be quite a laborious task unless the engineer has plenty of experience in seismic design using supplemental damping devices.

According to Sullivan et al. (2003), who evaluated the performance of eight different displacement-based seismic design procedures, most of the displacement-based design methods currently available successfully maintained the target design parameters even though significant variation in design strength existed. Recently the performance-based seismic design procedure has been applied to designing passive energy-dissipation devices: Kim et al. (2003) utilized the capacity spectrum method for seismic retrofit of existing structures using viscous dampers. Kim and Seo (2004) applied the direct displacement-based design procedure to design a structure with buckling-restrained braces. Lin et al. (2003) presented a displacement-based design method for new buildings with various passive devices. All of the above-mentioned studies verified the applicability of the proposed procedures by carrying out dynamic time-history analyses, and concluded that the nonlinear static procedures can be effective tools for seismic design of structures with passive energy dissipation devices.

In this study a nonlinear static analysis procedure of a structure is proposed using the displacement response spectrum and the capacity curve of the structure. The proposed procedure has similarity in concept with the capacity spectrum method presented in ATC-40, except that a displacement spectrum is used instead of an acceleration-displacement response spectrum. Then a procedure for evaluating the required amount of supplemental damping for seismic retrofit of existing structures is proposed utilizing the same displacement spectrum and the capacity curve used in the performance evaluation stage. Instead of relying on a trial and error process, the proposed method evaluates systematically the amount of supplemental dampers needed for the structure to satisfy the given performance objective. The proposed procedures for performance evaluation of structures and seismic design of

[1]Associate Professor, Dept. of Architectural Engineering, Sungkyunkwan Univ., Suwon 440-746, Korea (corresponding author). E-mail: jinkoo@skku.ac.kr

[2]Researcher, Institute of Science and Technology Research, Sungkyunkwan Univ., Suwon 440-746, Korea.

Note. Associate Editor: Sashi K. Kunnath. Discussion open until November 1, 2006. Separate discussions must be submitted for individual papers. To extend the closing date by one month, a written request must be filed with the ASCE Managing Editor. The manuscript for this paper was submitted for review and possible publication on April 11, 2002; approved on September 1, 2005. This paper is part of the ***Journal of Structural Engineering***, Vol. 132, No. 6, June 1, 2006. ©ASCE, ISSN 0733-9445/2006/6-873–883/$25.00.

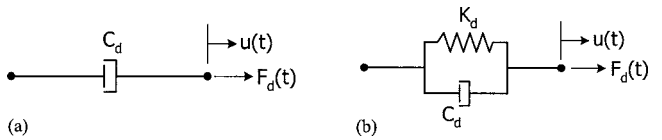

Fig. 1. Modeling of velocity-dependent devices

supplemental dampers are applied to ten- and 20-story steel structures, and the validity of the proposed methods are checked by nonlinear dynamic time-history analyses using artificial earthquake records generated based on the design spectrum.

Modeling of Supplemental Dampers

For analysis of structures with supplemental dampers various mathematical modeling techniques have been developed. Various models with increased complexity are reviewed in Reinhorn et al. (1995) for viscous dampers. Constantinou and Symans (1993) showed that the Maxwell model is adequate to capture the frequency dependence of the viscous dampers. It is also shown that, below a cutoff frequency of approximately 4 Hz, the model can be further simplified into a purely viscous dashpot model. It is stated in FEMA-274 (FEMA 1997b) that the damping force of a viscous damper can be modeled to be proportional to the velocity with a constant exponent ranging between 0.5 and 2.0. In preliminary analysis and design stages the velocity exponent of 1.0 is recommended for simplicity. In this study, based on those references, the behavior of viscous dampers is modeled by a linear dashpot.

A typical viscoelastic damper consists of thin layers of viscoelastic material bonded between steel plates. In practice the dynamic behavior of viscoelastic dampers is generally represented by a spring and a dashpot connected in parallel (Valles et al. 1996; Soong and Dargush 1997). For the linear spring-dashpot representation of the voscoelastic damper, the stiffness K_d and the damping coefficient C_d are obtained as follows:

$$K_d = \frac{G'(\omega)A}{t}$$

$$C_d = \frac{G''(\omega)A}{\omega t} \tag{1}$$

where $G'(\omega)$ and $G''(\omega)$=shear storage and shear loss moduli, respectively; A and t=total shear area and the thickness of the material, respectively; and ω=forcing frequency, for which the fundamental natural frequency of the structure is generally utilized in time domain analysis. With this spring-damper idealization the dynamic system matrices of the structure with added viscoelastic dampers can be constructed by superposing the damper properties to the stiffness and damping matrices of the structure. Fig. 1 represents the mathematical models of viscous and viscoelastic dampers employed in this study.

Performance Evaluation Using Displacement Spectrum and Capacity Curve

The direct displacement-based design (DBD), which focuses on displacement as the key design parameter, is considered to be an effective method for implementing performance-based seismic design utilizing deformation capacity and ductile detailing standards. In this study the general procedure of the DBD documented in the *SEAOC Blue Book* (SEAOC 1999) is applied in reverse order for evaluation of seismic performance of an existing structure. In principle the proposed analysis procedures are similar to the capacity spectrum method (CSM) (ATC 1996; FEMA 1997b; Freeman 1998) in that performance point is determined as a location where the displacement demand of the earthquake becomes equal to the plastic deformation capacity of the structure. The difference is on the use of displacement spectrum instead of the so called acceleration-displacement response spectrum (ADRS), therefore the extra work required for transforming the capacity and demand curves to ADRS format can be avoided. Although this may not be a significant improvement, it has the advantage of maintaining consistency with the proposed design procedure for supplemental dampers. Two nonlinear static analysis procedures, the step by step and the graphical procedure, which correspond to the nonlinear static procedure A and B of ATC-40, respectively, are proposed for seismic performance evaluation of structures (without dampers). The two procedures are summarized as in the following subsection.

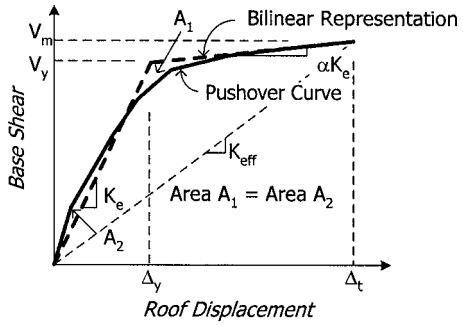

Fig. 2. Bilinear representation of pushover curve

Step by Step Procedure

1. Obtain base shear versus roof-story displacement capacity curve of a structure from pushover analysis.
2. Approximate the capacity curve by bilinear lines based on equal energy concept (area A_1=area A_2), and determine the quantities such as effective elastic stiffness, K_e, elastic natural period, T_e, base shear at yield, V_y, yield displacement, Δ_y, and postyield stiffness ratio, α (see Fig. 2).
3. Transform the roof-story displacement coordinate into pseudodisplacement coordinate, S_d, using the following relation:

$$S_d = \frac{\Delta_R}{\Gamma \phi_R} \tag{2}$$

where Δ_R=roof displacement, and Γ and ϕ_R=modal participation factor and the roof story component of the fundamental mode, respectively. This process corresponds to the transformation of the structure into an equivalent single degree of freedom (SDOF) structure.

4. Assume the first trial value for the maximum displacement, S_{dm}, of the equivalent structure, and determine the ductility factor, $\mu = S_{dm}/S_{dy}$. The equivalent damping ratio, ξ_{eq}, can be obtained as

$$\xi_{eq} = \frac{2(\mu - 1)(1 - \alpha)}{\pi\mu(1 + \alpha\mu - \alpha)} \quad (3)$$

Then the effective damping for the structure can be obtained as the sum of the equivalent damping and the inherent damping of the structure

$$\xi_{eff} = \xi_{eq} + \xi_i \quad (4)$$

where ξ_i=inherent damping, for which 5% of critical damping is generally utilized. Also the effective period, T_{eff}, corresponding to the maximum displacement can be obtained as

$$T_{eff} = T_e \sqrt{\frac{\mu}{1 + \alpha\mu - \alpha}} \quad (5)$$

where T_e=fundamental period of the structure.

5. Construct the displacement response spectrum for design earthquake using the effective damping obtained in the previous step, and read from the spectrum the next trial value for the maximum displacement S_{dm} corresponding to the effective period T_{eff}.
6. Repeat the process from Step 4 using the maximum displacement computed in the above step. Once the maximum displacement S_{dm} converges, then convert it into the maximum roof displacement using Eq. (2).
7. Carry out pushover analysis until the roof displacement reaches the maximum value computed above to estimate the maximum interstory drifts.

Graphical Procedure

1. Step 1–2. The same as those of the step by step procedure.
2. Step 3. Draw displacement response spectra with various damping ratios.
3. Step 4. For a series of ductility ratios, obtain maximum displacements ($S_{dm}=\mu\times S_{dy}$), effective periods $T_{eff}(\mu)$ [Eq. (5)], and effective damping ratios (ξ_{eff}) [Eq. (3) and (4)].
4. Step 5. Find out the point at which the effective damping ratio corresponding to a ductility ratio, obtained in Step 4, is equal to the equivalent damping ratio of a displacement spectrum crossing the point $[T_{eff}(\mu), S_{dm}(\mu)]$.
5. Step 6. Convert the maximum displacement computed in the above step into the maximum roof displacement, and carry out pushover analysis until the roof displacement reaches the maximum value computed above to estimate the maximum interstory drifts.

Design Procedure for Supplemental Dampers

If the maximum story drift of a structure subjected to a code-specified earthquake load exceeds the desired performance level, the structure needs to be retrofitted. Among the various methods for seismic retrofit, this study focuses on increasing damping to decrease earthquake-induced structural responses. To this end, a procedure for estimating the amount of supplemental damping required to satisfy the given performance objective is proposed. The basic idea is to compute the required damping from the difference between the total effective damping needed to meet the target displacement and the equivalent damping provided by the structure at the target displacement.

Required Damping to Meet Target Displacement

The damping ratio of the displacement response spectrum that intersects the point of the target displacement, S_{dt}, on the displacement ordinate (vertical axis) and the effective period, T_{eff}, on the period ordinate (horizontal axis) corresponds to the total effective damping, ξ_{eff}, for the structure to retain to meet the performance objective. For structures with supplemental dampers, the total effective damping is composed of the three components: inherent viscous damping, ξ_i, equivalent damping of the structure contributed from inelastic deformation of the structural members, ξ_{eq}, and the damping required to be added by the dampers, ξ_d.

The equivalent damping of the structure is obtained from the following equations (FEMA 1997b):

$$\xi_{eq} = \frac{1}{4\pi}\frac{E_{DS}}{E_S} = \frac{V_y S_{dt} - S_{dy} V_t}{\pi V_t S_{dt}} \quad \text{for VD} \quad (6a)$$

$$= \frac{V_{yd} S_{dt} - S_{dy} V_{td}}{\pi V_{td} S_{dt}} \quad \text{for VED} \quad (6b)$$

where $V_{yd}=V_y+K_d S_{dy}$, $V_{td}=V_t+K_d S_{dt}$, and E_S and E_{DS}=stored potential energy in the structure and the energy dissipated by hysteretic behavior of the structural members in the retrofitted structure, respectively.

Tsopelas et al. (1997) provides the contribution of the added damping to the total effective damping as $(\xi_d \times T_{eff})/T_e$ where ξ_d is the supplemental damping ratio. Then the required supplemental damping can be computed from the following equation:

$$\xi_d = (\xi_{eff} - \xi_{eq} - \xi_i)\frac{T_e}{T_{eff}} \quad (7)$$

where the total effective damping and the equivalent damping can be obtained from the displacement response spectrum and from Eq. (6), respectively.

Story-wise Distribution of Dampers

In multistory structures the supplemental damping computed in the equivalent SDOF system using Eq. (7) should be distributed throughout the stories of the original structure in such a way that the damping ratio for the fundamental vibrational mode becomes the required supplemental damping, ξ_d. For this purpose the

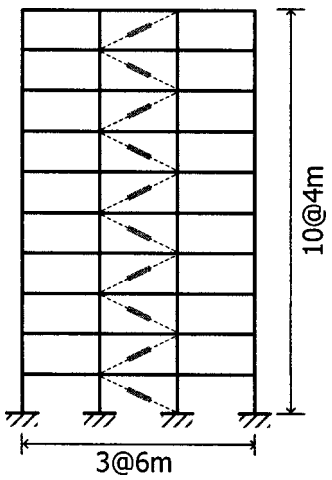

Fig. 3. Ten-story model structure for implementation of proposed method

expression for equivalent damping, Eq. (6), is used again, except that the energy dissipated by the dampers, E_{DV}, is used in the numerator instead of E_{DS}

$$\xi_{eq} = \frac{1}{4\pi}\frac{E_{DV}}{E_S} \tag{8}$$

If the dampers are placed as diagonal members with the inclination θ, then the energy dissipated by the dampers can be expressed as follows (FEMA 1997b):

$$E_{DV} = \frac{2\pi^2}{T_{eff,d}}\sum_{i=1}^{N} C_{di}\cos^2\theta_i(\Delta_i - \Delta_{i-1})^2 \tag{9}$$

where $T_{eff,d}$=secant period of the retrofitted structure; C_{di} and Δ_i=damping coefficient and the maximum lateral displacement of the ith story, respectively; and N=number of stories. The potential energy stored in the multistory structure can be expressed as follows:

$$E_S = \frac{2\pi^2}{T_{eff,d}^2}\sum_{i=1}^{N} m_i\Delta_i^2 \tag{10}$$

$$T_{eff,d} = 2\pi\sqrt{\frac{M^* S_{dt}}{V_y(1+\alpha\mu-\alpha)}} \quad \text{for VD} \tag{11a}$$

$$T_{eff,d} = 2\pi\sqrt{\frac{M^* S_{dt}}{V_y(1+\alpha\mu-\alpha)+K_d S_{dt}}} \quad \text{for VED} \tag{11b}$$

where M^*=effective modal mass and m_i=mass of the ith story. By substituting Eqs. (9) and (10) into Eq. (8), the damping ratio contributed from the dampers can be expressed as

$$\xi_d = \frac{1}{4\pi}\frac{T_{eff,d}\sum_{i=1}^{N} C_{di}\cos^2\theta_i(\Delta_i-\Delta_{i-1})^2}{\sum_{i=1}^{N} m_i\Delta_i^2} \tag{12}$$

In Eq. (12) the left-hand side of the equation, ξ_d, is obtained from Eq. (7) in the equivalent SDOF system. For VD the damping coefficient of the damper in the ith story, C_{di}, can be determined in Eq. (12), whereas for VED both C_{di} and K_{di} are the variables that should be determined. This can be done by using the relation $K_d=(G'/G'')\omega C_d$ obtained from Eq. (1). The simplest case is to assume that the dampers in all stories have the same capacity, and the damping coefficient in this case can be obtained from Eq. (12) as

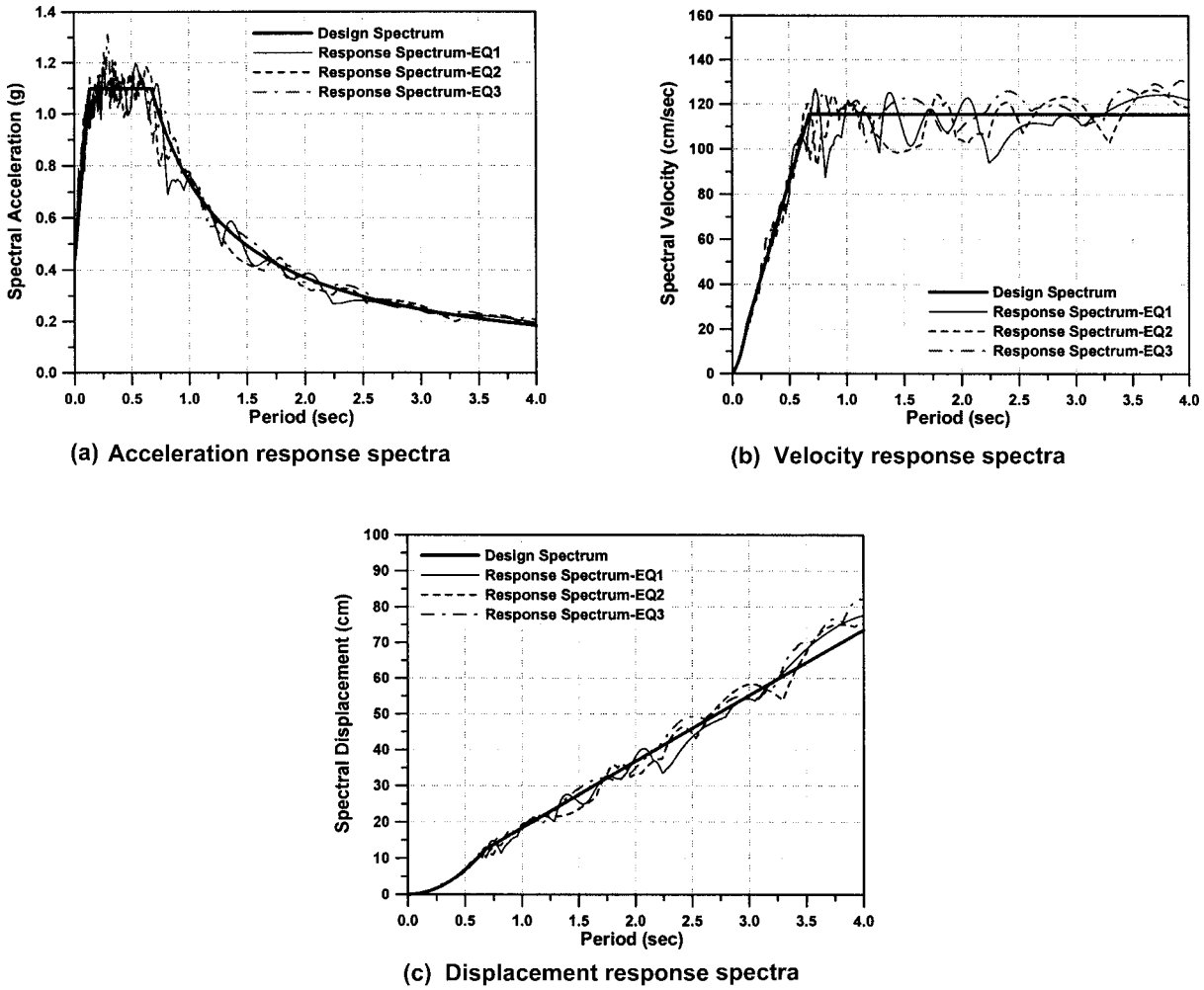

Fig. 4. Design and response spectra of input seismic loads (C_a=0.44, C_v=0.74)

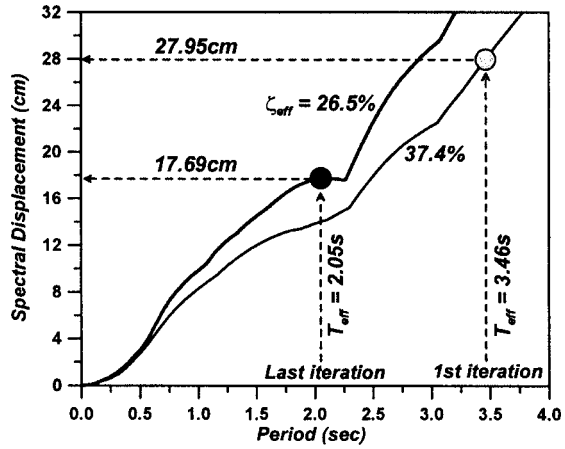

(a) Displacement response spectra (in equivalent SDOF system)

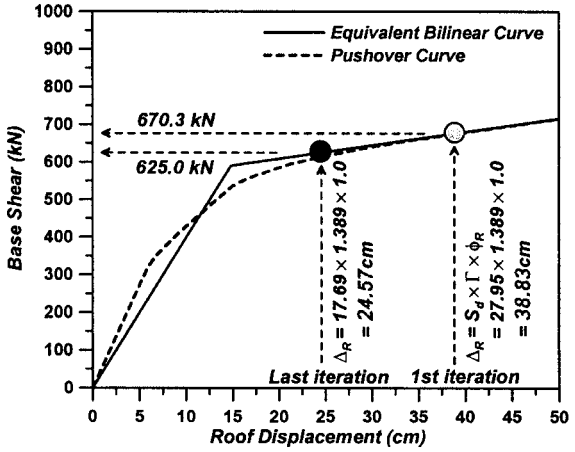

(b) Pushover curve (transformed into response of MDOF system)

Fig. 5. Evaluation of performance point of ten-story structure subjected to EQ-1 earthquake using step by step method

$$C_d = \frac{4\pi\xi_d \sum_{i=1}^{N} m_i \Delta_i^2}{T_{\text{eff},d} \sum_{i=1}^{N} \cos^2\theta_i (\Delta_i - \Delta_{i-1})^2} \tag{13}$$

In this stage, however, the maximum story displacements, except for the top-story displacement given as performance limit state,

Table 1. Evaluation of Performance Point of Ten-Story Structure Using Step by Step Procedure

Displacement (cm)	μ	ξ_{eff} (%)	T_{eff} (s)	Difference (%)
71.99	6.74	37.4	3.46	—
27.95	2.62	36.2	2.48	−157.60
18.08	1.69	27.3	2.07	−54.59
17.40	1.63	26.2	2.04	−3.91
17.80	1.67	26.9	2.06	2.25
17.54	1.64	26.4	2.05	−1.50
17.72	1.66	26.7	2.06	1.04
17.61	1.65	**26.5**	2.05	−0.63
17.69	1.66	—	**2.05**	0.42

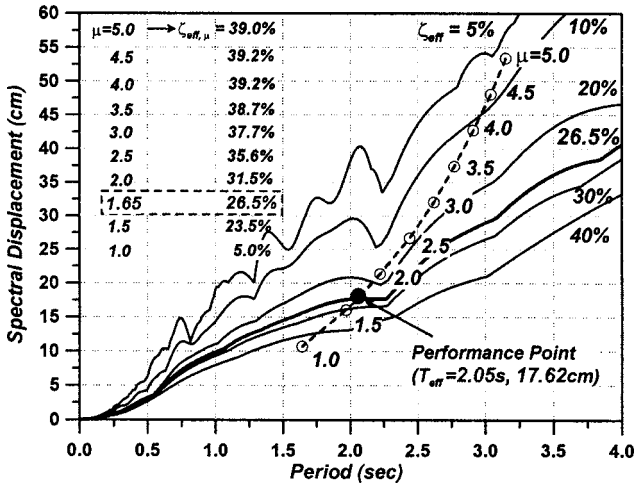

Fig. 6. Evaluation of performance points of ten-story structure subjected to EQ-1 earthquake using graphical method

are unknown. Therefore the configuration for lateral story drifts Δ_i needs to be assumed in Eq. (12) and (13). A simple case is to assume that the maximum story drifts are proportional to the fundamental mode shape or to the pushover curve. The story-wise distribution pattern for the dampers also needs to be assumed.

For viscous dampers the design process ends here; however for dampers with stiffness, such as viscoelastic or hysteretic dampers, iteration is required because the added dampers increase system stiffness. In that case the capacity curve of the system needs to be redrawn considering added dampers and the process is repeated until convergence.

Summary of Design Procedure

The proposed procedure to design supplemental dampers for performance-based seismic retrofit of existing structures can be summarized in the following steps:

1. Carry out eigenvalue analysis of the structure to obtain natural periods and mode shapes. Using the mode shapes, perform pushover analysis to obtain top story versus base shear curve, and transform the pushover curve into a capacity curve using Eq. (2). Idealize the curve into a bilinear shape and read the yield displacement, S_{dy}.
2. Decide a desired target roof displacement, and transform it into the target value in the equivalent SDOF system, S_{dt}. Obtain ductility ratio, $\mu S_{\text{dt}}/S_{\text{dy}}$, the effective period, T_{eff} [Eq. (5)], and the equivalent damping ξ_{eq} [Eq. (6)] at the target displacement.
3. Find out the effective damping ratio corresponding to the displacement response spectrum that crosses the point of the target displacement and the effective period. This corresponds to the total demand on damping imposed by the earthquake. It would be more convenient to start the procedure with response spectra with various damping ratios.
4. Compute the required damping for supplemental dampers from Eq. (7).
5. The required damping is distributed throughout the stories using Eq. (12). The size of dampers in each story is designed based on the required damping allocated to the story.
6. For structures retrofitted with VED, carry out eigenvalue analysis and redraw the capacity curve of the structure using

Table 2. Structural Responses Obtained from Static and Dynamic Analyses

Model	Artificial earthquake records	Equivalent SDOF system displacement (cm)	MDOF system		Effective damping (%)	Time history analysis result displacement (cm)
			Displacement (cm)	Base shear (kN)		
10 story	EQ-1	17.69	24.57	625.0	26.5	23.89
	EQ-2	17.50	24.31	624.1	26.2	26.07
	EQ-3	17.90	24.86	626.0	26.9	25.48
20 story	EQ-1	42.95	62.19	739.7	25.6	62.78
	EQ-2	42.19	61.10	738.5	24.8	66.11
	EQ-3	36.66	53.08	729.8	19.6	52.26

the newly obtained mode shape, and repeat from Step 1 until convergence.

7. Check whether the structural members, especially columns, can resist the additional axial and shear forces imposed by dampers. If necessary, structural members are reinforced.

Application to Multistory Structures

Model Structures and Earthquake Loads

For verification of the proposed method, ten- and 20-story steel rigid frames designed in accordance with the Korean design code for gravity and wind loads are prepared. For gravity load uniform dead load of 5.30 kPa and live load of 2.45 kPa are applied throughout the stories. Basic wind speed of 35 m/s is used for lateral static wind load. The yield stress of the structural steel is 235 and 323 MPa for beams and columns, respectively. Fig. 3 shows the ten-story structure with supplemental dampers. The 20-story structure has the same bay width and story height. The sectional dimensions and the dynamic modal characteristics of the model structures can be found in Kim et al. (2003).

Elastic design response spectra, shown in Fig. 4, are constructed in accordance with the *Korean seismic design guidelines* (EESK 1997) for earthquakes with a recurrence period of 2,400 years on soil profile type S_E (weak soil). Based on the design spectrum, three artificial time history records are generated using the program *SIMQKE* (Vanmarcke and Gasparini 1976) for verification of the static procedure by carrying out nonlinear dynamic time-history analyses. The response spectra constructed from the time-history records are also plotted in Fig. 4, where it can be observed that the response spectra match the design spectrum very well.

Performance Evaluation

The seismic performances of the model structures for given seismic load are evaluated by the nonlinear static analysis procedure proposed previously. It is assumed that the structural members show a bilinear force-deformation relationship with the postyield stiffness of 3% of the initial stiffness, and that the plastic hinges form as point hinges. Pushover analysis is carried out using the program code Drain-2D+ (Tsai and Li 1997) with static story forces proportional to the equivalent mode shape (Valles et al.1996) computed using the following equation:

$$F_i = \frac{m_i \bar{\Phi}_i}{\sum_{i=1}^{N} m_i \bar{\Phi}_i} V \tag{14a}$$

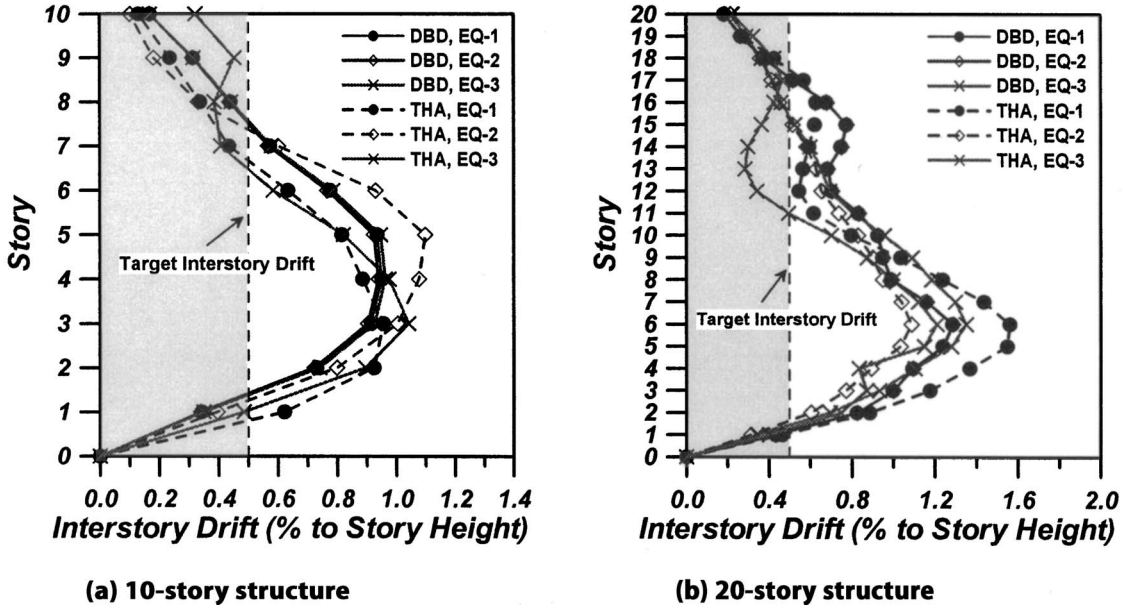

Fig. 7. Maximum interstory drifts of model structures

Table 3. Estimation of Required Damping in Ten-Story Structure Subjected to EQ-1 Earthquake

Target displacement (cm)	ξ_{eff} (%)	T_{eff} (s)	T_e (s)	ξ_d (%)	C_d (kN s/cm)	K_d (kN/cm)	Difference (%)
14.4	34.1	1.877	1.642	12.76	3.72	14.22	—
	29.4	1.626	1.466	12.19	3.98	17.05	−15.46
	28.6	1.587	1.437	11.99	3.99	17.44	−2.46
	28.5	1.582	1.433	**11.97**	3.99	17.50	−0.33

$$\bar{\phi}_i = \sqrt{\sum_{i=1}^{N} (\phi_{ij}\Gamma_j)^2}$$

$$\Gamma_j = \frac{\sum_{i=1}^{N} m_i \phi_{ij}}{\sum_{i=1}^{N} m_i \phi_{ij}^2} \tag{14b}$$

where F_i=seismic story force of the ith floor; m_i=mass of the ith floor; ϕ_{ij}=ith component of the jth mode shape vector; V=base shear; and N=number of stories.

The pushover curves are fitted to the bilinear lines as shown in Fig. 2, and the effective elastic stiffness K_e, displacement at yield S_{dy}, and the base shear at yield V_y are obtained. The initial performance point is assumed to be 2.5% of the structure height, which is 100 and 200 cm for ten- and 20-story structures, respectively. Fig. 5 and Table 1 present the procedure for performance evaluation of the ten-story model structure using the step by step method. The ratio of the yielded stiffness to the elastic stiffness, the yield displacement, and yield base shear of the original structure, turn out to be 0.0905, 14.83 cm, and 589.9 kN, respectively. The results from the graphical method are presented in Fig. 6, where it can be observed that the maximum displacements obtained from the two methods are almost identical. The results from the nonlinear static procedures are compared with those from the time-history analyses in Table 2, which show that the maximum top-story displacements obtained from the static procedures slightly underestimate those from time-history analyses. The difference ranges from 2.43 to 6.75% for the ten-story structure and from 0.94 to 7.57% for the 20-story structure.

Estimation of Required Supplemental Damping

The amount of the supplemental damping required to limit the maximum displacement within the target displacement is obtained following the proposed procedure. The target interstory drift is set to be 0.5% of the story height, which corresponds to the "functional" limit state recommended in the *SEAOC Blue Book* (SEAOC 1999). This results in the target roof displacement of 20 and 40 cm for the ten- and 20-story structures, respectively. It can be noticed in Fig. 7 that story drifts of more than half of the stories exceed the target interstory drift. Table 3 presents the procedure for evaluation of damping for VD and VED required for the ten-story structure to satisfy the given performance limit state. C_d and K_d are the damping coefficient and the stiffness of VED in the equivalent SDOF system. The target roof displacement of the ten-story structure, which is 20 cm, is transformed to 14.4 cm in the equivalent SDOF system. The amount of relevant damping for VD and VED are presented in Tables 4(a) and (b), respectively. From the results it can be observed that the required damping for VED is smaller than that for VD, which is due to the inherent stiffness of VED.

Distribution of Supplemental Dampers

The required amount of supplemental damping evaluated for the equivalent SDOF system needs to be properly distributed throughout the stories of the original structure. In this study Eq. (13) is used for story-wise distribution of supplemental dampers, and the following four cases are investigated. The story drift Δ_i is obtained from the pushover curve:

Table 4. Required Damping of Different Earthquake Loads

Number of stories	Artificial earthquake records	T_e (s)	T_{eff} (s)	ξ_{eff} (%)	ξ_d (%)
	(a) Structures with viscous dampers				
10	EQ-1	1.642	1.877	34.1	12.8
	EQ-2			34.3	12.9
	EQ-3			35.7	14.2
20	EQ-1	3.362	3.362	35.3	30.3
	EQ-2			32.5	27.5
	EQ-3			22.8	17.8
	(b) Structures with viscoelastic dampers				
10	EQ-1	1.433	1.582	28.5	12.0
	EQ-2	1.495	1.666	26.1	8.7
	EQ-3	1.453	1.609	27.6	10.8
20	EQ-1	2.679	2.679	23.2	18.2
	EQ-2	2.856	2.856	19.0	14.0
	EQ-3	2.805	2.805	20.4	15.4

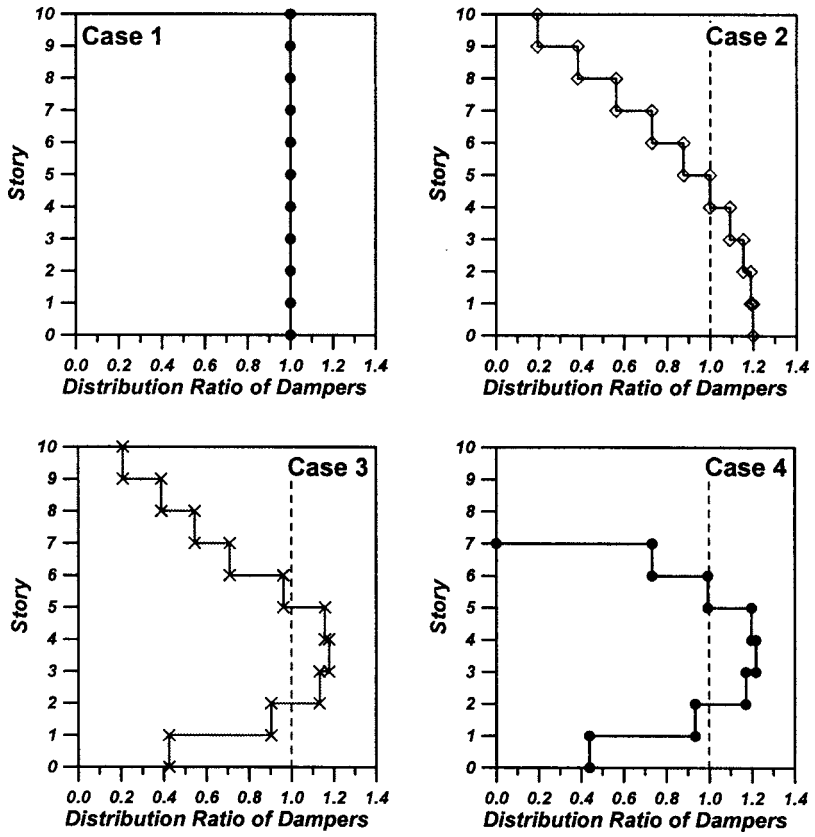

Fig. 8. Story-wise distribution patterns for supplemental dampers in ten-story structure

1. Case 1: Dampers are uniformly distributed in all stories (i.e., C_{di} is constant in all stories).
2. Case 2: Damper size in the jth story is proportional to the story displacements accumulated from the top story to the jth story ($\Sigma_{i=j}^{N}\Delta_i/\Sigma_{i=1}^{N}\Delta_i$).
3. Case 3: Damper size in each story is proportional to the interstory drifts.
4. Case 4: The same with the Case 3 except that dampers are installed only in lower stories where interstory drifts exceed the target drift.

The story-wise distribution patterns are illustrated graphically in Fig. 8. Table 5 presents the ratios of the maximum top-story displacements of the model structures with added dampers and the given target displacements. Also shown are the total damping coefficients of the dampers distributed in accordance with the methods mentioned above. According to the analysis results the structures retrofitted with both dampers generally satisfy the given performance limit state. The correspondence between the target and the maximum displacement is better in the structure installed with viscous dampers. The discrepancy is largest in the 20-story structure retrofitted with VED, where the maximum displacements exceed the target by as much as 23%.

It can be noticed that the total amount of added damping required to meet the same target displacement varies depending on the distribution pattern for added dampers; Table 5 shows that the sums of damping coefficients in the Case 2 story-wise damper distribution are 16 and 24% smaller than those in the Case 1 distribution for the ten-and the 20-story structures, respectively, and that those in Case 3 are 24 and 31% smaller for the ten-story and the 20-story structures, respectively, while the maximum displacements increase only by 1–7%. It can be observed in Fig. 7 that in approximately the upper third of the stories, the interstory drifts are less than 0.5% of the story height. Therefore it would be more economical to install supplemental dampers in lower stories with large interstory drift (Case 4). For the ten-story structure subjected to the EQ-1 earthquake, the total damping coefficient results in 147.9 kN s/cm, which corresponds to only 67% of the Case 1 distribution, while the maximum displacement increases only 1.2% compared with Case 1 distribution. Similar results can be observed in the 20-story structure and for other earthquake loads.

Iteration of Design Process

When a structure is retrofitted with VED, the static and dynamic characteristics change mostly due to the added stiffness. However in the mode shapes and the capacity curve used in the initial design process, this change is not reflected. This results in the relatively large discrepancy between the maximum displacement and the target value of the structure with VED, especially in the 20-story structure. Therefore the accuracy of the proposed method would be enhanced if another eigenvalue analysis and pushover analysis are carried out with the structure installed with VED and the whole design procedure is repeated with the newly obtained mode shapes and dynamic characteristics. Fig. 9 plots the pushover curve and Table 6 presents the modal characteristics of the 20-story structure before and after it is retrofitted with VED following the Case 4 distribution pattern. This example is chosen because it shows the largest discrepancy between the maximum and the target displacements. It can be observed that after the VEDs are installed, the elastic period decreases and the ultimate strength and both the elastic and postelastic stiffness increase as a

Table 5. Summation of Damping Coefficients and Ratio of Maximum to Target Displacement for Each Damper Distribution Pattern

Number of stories	Distribution patterns	Artificial earthquake records					
		2EQ-1		EQ-2		EQ-3	
		ΣC_{di}	$\frac{u_{max}}{u_r}$	ΣC_{di}	$\frac{u_{max}}{u_t}$	ΣC_{di}	$\frac{u_{max}}{u_t}$
		(a) Structures with viscous dampers (ΣC_{di}) (kN s/cm)					
10	Case 1	221.0	0.97	224.1	1.05	245.5	0.91
	Case 2	185.1	0.99	187.7	1.05	205.3	0.92
	Case 3	168.1	0.99	170.7	1.06	186.5	0.92
	Case4	147.8	1.01	150.0	1.13	164.0	0.93
20	Case 1	2,302.8	0.94	2,046.8	0.93	1,334.1	1.02
	Case 2	1,896.9	0.97	1,633.1	0.98	1,096.8	1.06
	Case 3	1,844.1	0.97	1,491.7	0.99	1,048.9	1.06
	Case 4	1,756.9	0.99	1,343.3	1.04	938.9	1.09
		(b) Structures with viscoelastic dampers (ΣC_{di}) (kN s/cm)					
10	Case 1	245.9	0.99	169.5	1.04	2,18.4	0.92
	Case 2	205.9	1.02	141.9	1.05	182.7	0.97
	Case 3	187.1	1.03	129.1	1.06	166.0	0.95
	Case 4	164.4	1.10	113.4	1.07	146.0	1.00
20	Case 1	1,735.8	1.21	1,226.6	1.12	1,383.3	1.07
	Case 2	1,429.8	1.23	978.6	1.15	1,137.3	1.12
	Case 3	1,390.0	1.23	893.9	1.19	1,087.6	1.11
	Case 4	1,324.2	1.23	805.0	1.21	973.6	1.17

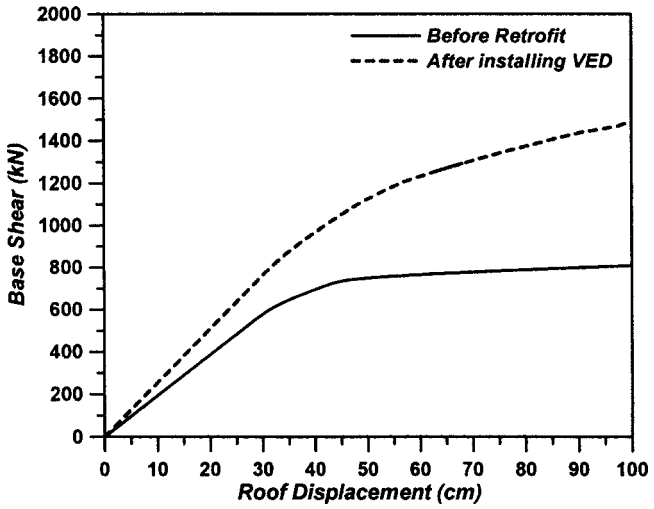

Fig. 9. Pushover curves of 20-story structure before and after retrofit

result of the added stiffness. The modal participation factor and the effective mass are not varied significantly. It is also shown that the maximum displacement of the structure decreases from 49.24 to 42.57 cm, which is much closer to the target displacement of 40 cm, when the design process of VED is applied again using the new mode shape and the new capacity curve.

Examination of Member Forces Induced by Dampers

Fig. 10 shows the change in story shear of the ten-story structure subjected to the EQ-1 earthquake before and after it is retrofitted by supplemental dampers. The base shear of the structure retrofitted with viscous dampers increased only 3–8%. In the case of the structure retrofitted by VED, however, the base shear increased 14–15% depending on the story-wise damper distribution patterns. The increase in the base shear results mainly from the input seismic energy magnified by the increased stiffness. Fig. 11 depicts the change in the axial force of the interior columns due to the installation of the dampers. It can be observed that the installation of the supplemental dampers significantly increases the axial force of the interior columns, where dampers are connected.

Table 6. Redesign of 20-Story Structure with VED (Case 4) Subjected to EQ-1 Earthquake

	Elastic period T_e (s)	Modal participation Factor (Γ)[a]	Effective mass M^* (%)[a]	Postyield stiffness ratio (α)	Maximum displacement u_{max} (cm)
Before retrofit	3.24	1.448	84.4	0.061	49.24[b]
After retrofit	2.80	1.493	84.2	0.278	42.57[c]

[a]Equivalent mode is used.

[b]Displacement of the structure with VED designed using dynamic characteristics of the original structure.

[c]Displacement of the structure with VED designed using dynamics characteristics of the retrofitted structure.

It is interesting to note that the axial force of the columns connected to viscous dampers also increases even though the story shear forces do not change significantly. This can be explained by the fact that the axial force of the exterior columns, where the dampers are not connected, rather decreases after the dampers are installed. This implies that when dampers are installed the member forces are redistributed, and therefore it would be necessary to check if the structural members, especially columns and footings, can resist the additional member forces. If it turns out that the members are not strong enough to sustain the additional member forces, the members should be properly reinforced before the dampers are installed.

Conclusion

In this study a nonlinear static procedure for seismic performance evaluation of structures was developed using the displacement response spectrum and the capacity curve. Then a procedure for determining the amount of velocity-dependent energy dissipation devices required to meet a given target displacement was proposed. The performance of the model structures retrofitted by the proposed method was evaluated by nonlinear time-history analysis to determine whether the given performance objective was satisfied.

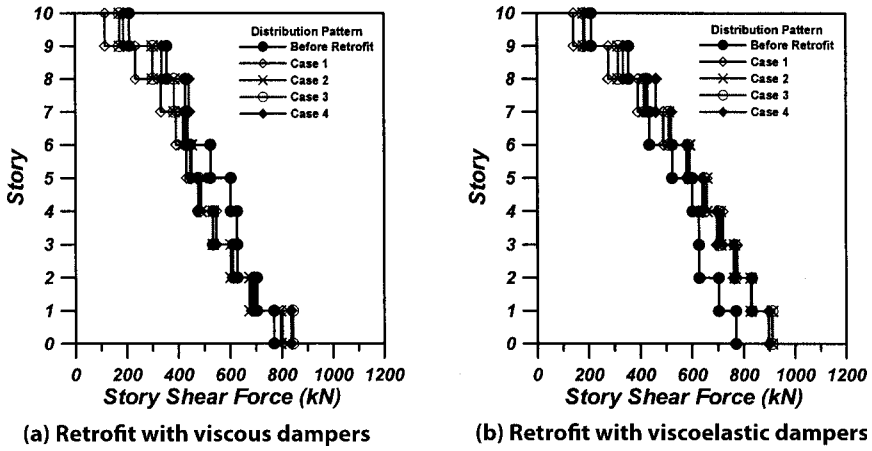

Fig. 10. Maximum story shear of ten-story structure subjected to EQ-1 earthquake

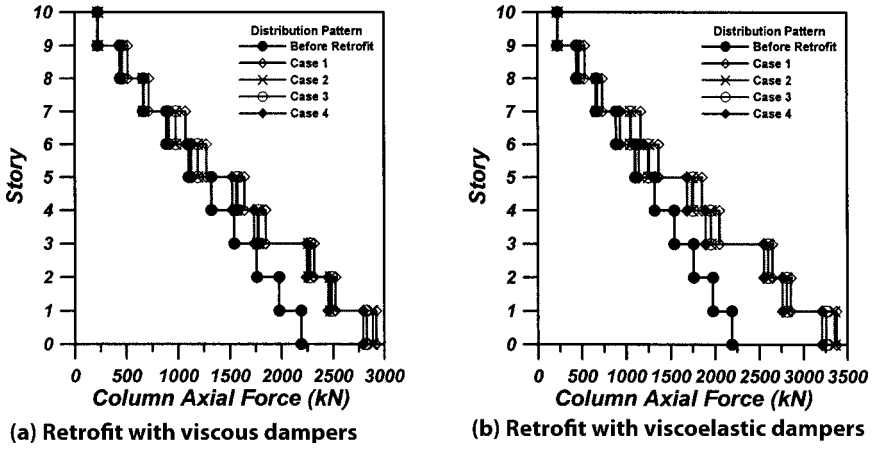

Fig. 11. Maximum axial force in interior columns of ten-story structure subjected to EQ-1 earthquake

The analysis results confirmed that both the step-by-step method and the graphical method produced the same performance points, and that the nonlinear static analysis results were compatible with those from time-history analyses. It is also shown that the maximum displacements of the model structures retrofitted by supplemental dampers were close to the given target displacement. Among the story-wise distribution patterns for dampers, the distribution of dampers only in the lower two thirds of stories proportional to the interstory drift turned out to be the most effective.

The analysis results verified that the proposed method could be a potential tool for simplified nonlinear static analysis of structures and for performance-based retrofit of existing structures using velocity-dependent supplemental dampers. However it should be mentioned that the proposed process inherits the generic limitations of the nonlinear static analysis procedure. FEMA-356 (FEMA 2000) recommends that the nonlinear static procedure should not be used for structures in which higher mode effects are significant. Further discussion on this issue can be found in Krawinkler (1995) and Fajfar (2000).

Acknowledgments

This research (Grant No. C105A1050001-05A0505-00210) was financially supported by the Ministry of Construction and Transportation of South Korea, and Korea Institute of Construction and Transportation Technology Evaluation and Planning. The writers are grateful to the authorities for their support.

References

Applied Technology Council (ATC). (1996). "Seismic evaluation and retrofit of concrete buildings." *ATC-40*, Redwood City, Calif.

Constantinou, M. C., and Symans, M. D. (1993). "Experimental study of seismic response of buildings with supplemental fluid dampers." *Struct. Des. Tall Build.*, 2(2), 93–132.

Earthquake Engineering Society of Korea (EESK). (1997). *Seismic design guidelines II*, Ministry of Construction and Transportation, Seoul, Korea.

Fajfar, P. (2000). "A nonlinear analysis method for performance-based seismic design." *Earthquake Spectra*, 16(3), 573–592.

Federal Emergency Management Agency (FEMA). (1997a). "NEHRP guidelines for the seismic rehabilitation of buildings." *FEMA-273*, Prepared by the Applied Technology Council for the Building Seismic Safety Council, Washington, D.C.

Federal Emergency Management Agency (FEMA). (1997b). "NEHRP commentary on the guidelines for the seismic rehabilitation of buildings." *FEMA-274*, Prepared by the Applied Technology Council for the Building Seismic Safety Council, Washington, D.C.

Federal Emergency Management Agency (FEMA). (2000). "Prestandard and commentary for the seismic rehabilitation of buildings." *FEMA-356*, Prepared by the American Society of Civil Engineers for the Federal Emergency Management Agency, Washington, D.C.

Freeman, S. A. (1998). "Development and use of capacity spectrum method." *Proc., 6th National Conf. on Earthquake Engineering*, Seattle.

Kim, J. K., Choi, H. H., and Min, K. W. (2003). "Performance-based design of added viscous dampers using capacity spectrum method." *J. Earthquake Eng.*, 7(1), 1–24.

Kim, J. K., and Seo, Y. I. (2004). "Seismic design of low-rise steel frames with buckling-restrained braces." *Eng. Struct.*, 26(5), 543–551.

Krawinkler, H. (1995). "New trends in seismic design methodology." *Proc., 10th European Conf. on Earthquake Engineering*, Vienna, Austria.

Lin, Y. Y., Tsai, M. H., Hwang, J. S., and Chang, K. C. (2003). "Direct displacement-based design for building with passive energy dissipation systems." *Eng. Struct.*, 25(1), 25–37.

Reinhorn, A. M., Li, C., and Constantinou, M. C. (1995). "Experimental and analytical investigation of seismic retrofit of structures with supplemental damping, Part I: Fluid viscous damping devices." *Technical Rep. NCEER-95-0001*, National Center for Earthquake Engineering Research, Buffalo, N.Y.

Soong, T. T., and Dargush, G. F. (1997). *Passive energy dissipation systems in structural engineering*, Wiley, New York.

Structural Engineers Association of California (SEAOC). (1999). *Recommended lateral force requirements and commentary*, Appendix I, Sacramento, Calif.

Sullivan, T. J., Calvi, G. M., Priestley, M. J. N., and Kowalsky, M. J. (2003). "The limitations and performances of different displacement based design methods." *J. Earthquake Eng.*, 7(1), 201–241.

Tsai, K. C., and Li, J. W. (1997). "DRAIN2D+, A general purpose computer program for static and dynamic analyses of inelastic 2D structures supplemented with a graphic processor." *Rep. CEER/R86-07*, National Taiwan Univ., Taipei, Taiwan.

Tsopelas, P., Constantinou, M. C., Kircher, C. A., and Whittaker, A. S. (1997). "Evaluation of simplified method of analysis for yielding structures." *Technical Rep. NCEER-97-0012*, National Center for Earthquake Engineering Research, State Univ. of New York at Buffalo, Buffalo, N.Y.

Valles, R. E., Reinhorn, A. M., Kunnath, S. K., Li, C., and Madan, A. (1996). "IDARC 2D version 4.0: A computer program for the inelastic damage analysis of buildings." *Technical Rep. NCEER-96-0010*, National Center for Earthquake Engineering Research, State Univ. of New York at Buffalo, Buffalo, N.Y.

Vanmarcke, E. H., and Gasparini, D. A. (1976). *A program for artificial motion generation, Users manual and documentation*, Dept. of Civil Engineering, Massachusetts Institute of Technology, Cambridge, Mass.